

ABSOLUTE AND CONVECTIVE INSTABILITY OF A LIQUID JET

S. P. Lin,¹ M. Hudman² and J. N. Chen^{3, 1,2,3} Clarkson University, Potsdam, NY 13699.

ABSTRACT

The existence of absolute instability in a liquid jet has been predicted for some time (ref. 1-5). The disturbance grows in time and propagates both upstream and downstream in an absolutely unstable liquid jet. The image of absolute instability is captured in the NASA 2.2 sec drop tower, and is reported here. The transition from convective to absolute instability is observed experimentally. The experimental results are compared with the theoretical predictions on the transition Weber number as functions of the Reynolds number. The role of interfacial shear relative to all other relevant forces which cause the onset of jet breakup had not been quantitatively elucidated before (ref. 6), and is explained here.

IMAGE OF ABSOLUTE INSTABILITY

The commonly observed manifestation of the onset of instability in a liquid jet with a sufficiently large velocity is the amplification of disturbances



Figure 1: A Convectively Unstable Jet. $We = 100$,
 $Re = 160$

which are convected downstream to break up the jet into drops. The observed instability belongs to a general class of instability called convective instability which allows the disturbance to be convected only in the downstream direction. The literature on convective instability is very rich, and is reviewed in many articles including the most recent ones by Chiegar and Reitz (ref. 7), Lin (ref. 8), Lin and Reitz (ref. 6). There exists another class of instability called absolute instability which permits the disturbance to propagate in both the downstream and upstream directions. This class of instability is less well studied. Leib and Goldstein (refs. 1-2) were the first to demonstrate that, in absence of gravity and ambient gas, a liquid jet with a relatively small velocity may become absolutely unstable due to surface tension force. Even in the presence of gas, with (ref. 4) or without gas viscosity (ref. 3) or compressibility (ref. 5), absolute instability still occurs. However the physical appearance of a liquid jet which suffers the consequence of absolute instability without the interference of gravity has been obtained only recently (ref. 9). The fact that the photographs indeed give evidence of absolute instability is substantiated by the delineation of transition from convective to absolute instability observed in the NASA Lewis 2.2 second drop tower.

The detailed description of the equipment and procedure used for the experiments are available (ref. 9-10), and will not be reproduced here. The entire system was housed in a drop rig of dimension 41.4 cm x 40.6 cm x 81.2 cm, and of weight 152.4kg. The rig attained 10^{-4} g in the NASA 2.2 second drop tower, and survived 30 g impacts for more than 100 drops. Glycerin and water mixtures, SAE 10 oil, and silicon oil were used as test fluids.

Figure 1 is a photograph (ref. 9, 10) of a convectively unstable glycerin and water jet in air at $We = 100$, $Re = 160$. Re and We are the Reynolds and Weber numbers respectively defined by

$$Re = \frac{Ua}{\nu}, We = \frac{\rho U^2 a}{S}$$

where U is the average jet velocity, a is the nozzle radius, ν is the liquid kinematic viscosity, S is the surface tension, and ρ is the liquid density. The dimensionless wave number, defined as the ratio of $2\pi a$ and the wavelength, is 0.66 ± 0.025 based on the

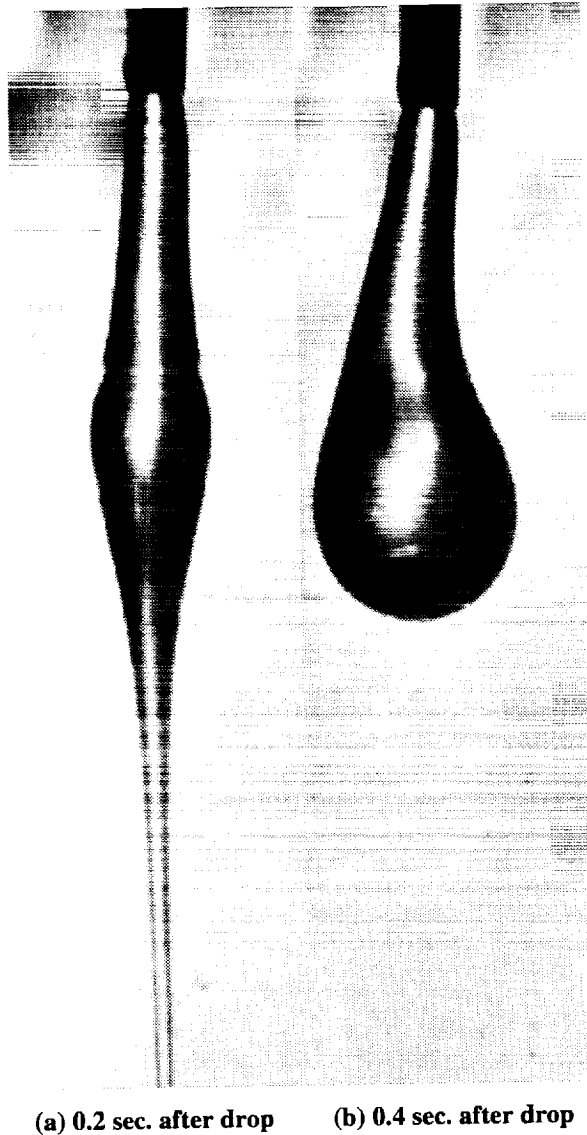


Figure 2: An Absolutely Unstable Liquid Jet.
($We=0.349$, $Re=0.082$)

wavelength appearing in this figure. The observed wave number is close to 0.697 corresponding to the most amplified waves according to the Rayleigh theory. It will be shown presently that as the Weber number is decreased to lie below a critical number which is a function of other flow parameters, the convectively unstable jet suddenly becomes absolutely unstable. The onset of absolute instability has a totally different consequence. In contrast to the case of a convectively unstable jet, the disturbance in an absolutely unstable jet was observed to propagate not only in the downstream direction but also in the upstream direction, as predicted by theory.

Figures 2(a) and 2(b) are the photographs (ref. 9, 11) of a glycerin jet which give an example of

absolute instability. They were taken at 0.2 sec and 0.4 sec after the test rig was dropped in the drop tower. Right after the onset of absolute instability, the upstream propagating disturbance suddenly rushed toward the nozzle tip to form a pendant while the downstream propagating disturbance grows slowly along the thin thread of liquid downstream of the forming pendant. Between 0.2 sec and 0.4 sec after the rig was dropped the liquid thread is pinched off by the pendant and washed out of the view of the camera. It appears that the physical mechanism of absolute instability remains capillary pinching as predicted by theory (ref. 12). Note also that the disturbance amplitude grows temporally everywhere along the jet after the onset of absolute instability. Thus the observed mode of instability appears to be the global absolute instability in the sense of Huerre and Monkewitz (ref. 13). The nonlinear evolution of absolute instability in a liquid jet was conjectured earlier (refs. 3, 14) to lead to a dripping jet. A dripping jet was not observed during the 2.2 seconds in the drop tower. Instead the pendant near the nozzle tip grew in volume and became more spherical in shape as the flow through the nozzle was kept constant at microgravity. It is not known if a dripping jet observed (ref. 14) on earth will also be encountered if the duration of the free fall of the test rig is much longer than 2.2 sec.

The transition from convective instability to absolute instability at different Reynolds numbers were observed. The results of the observation are given in Fig. 3. The experimental points obtained with glycerin are shown in circles, and that obtained with silicone oil are shown in squares. The uncertainties associated with Re and We are indicated respectively with horizontal and vertical error bars. For the experimental points without error bars, the length of the error bars are shorter than the diameter of the circles or the diagonal of the squares. The open circles and squares represent convective instability and the filled ones represent absolute instability. It is seen in Fig. 3 that as the velocity of a silicone oil jet corresponding to the open square with the largest values of Re and We is reduced in the successive 5 drop tower tests represented by the 5 open squares, the appearance of the jet remains that depicted in Fig. 1. Thus the jet with the values of Re and We indicated by the open squares remains convectively unstable. Further reduction in the jet velocity in the subsequent ten drop tower tests represented by the filled squares changes the appearance of the jet to that depicted in Fig. 2. Thus the jet becomes absolutely unstable at the critical set (Re_c , We_c) in the $Re - We$ parameter space between the nearest open and filled squares, and remains

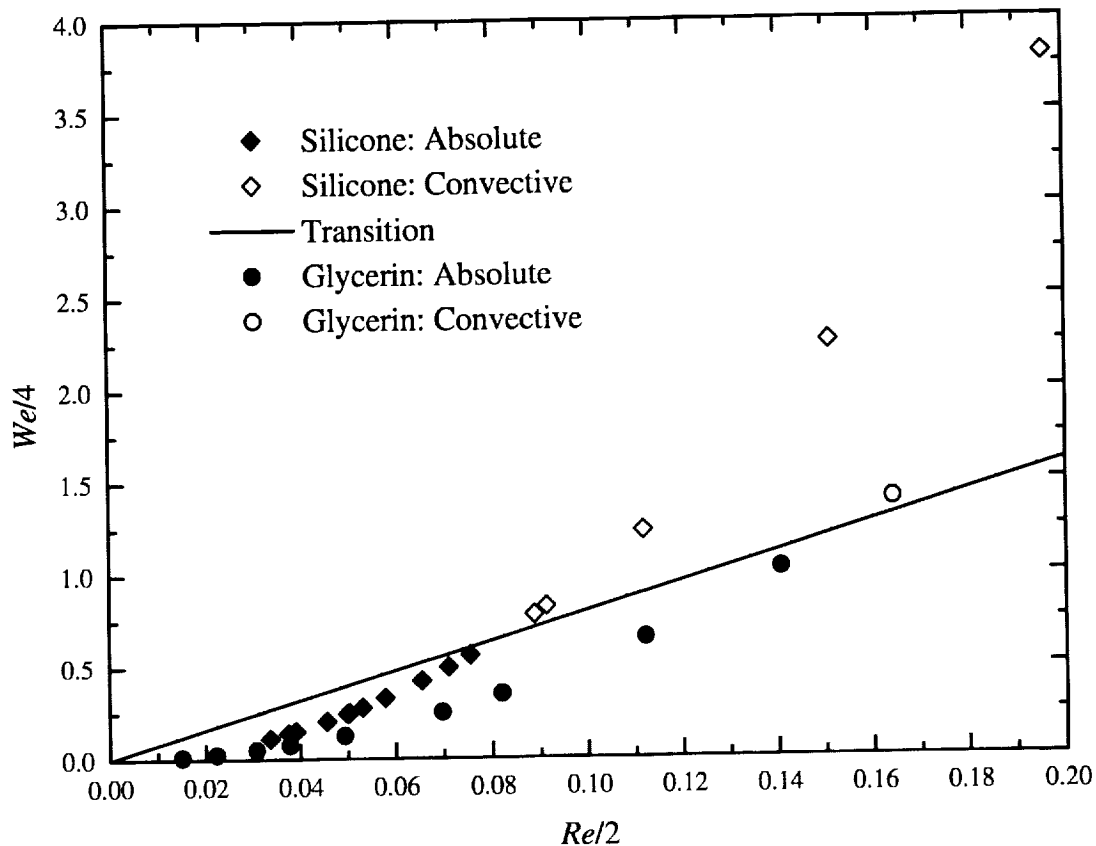


Figure 3: Transition from absolute to convective instability

absolutely unstable in the ten tests with the values of (Re, We) smaller than (Re_c, We_c) . Similar results are shown in circles for a glycerin jet. The transition occurs between the nearest open and filled circles at larger values of Re and We for the glycerin jet. When the nearest open and filled circles are connected with a straight line, it happens to pass through the nearest open and filled squares and also through the origin. This is quite reasonable, since in the theoretical prediction (refs. 1-5) the transition curve in the region of small (Re, We) is almost a straight line. However, the known theoretical predictions have not been able to extend the transition curve all way to the origin due to the difficulty involved in attaining a sufficient numerical accuracy. In fact the values of Re in Fig. 3 are already so small that no accurate numerical results are available for direct comparisons on the transition curve depicted in the figure. Although a quantitative comparison between theory and experiment is not yet possible (ref. 9), the observed qualitative trends that

the critical Weber numbers of transition decrease with Reynolds numbers and that the jet is convectively or absolutely unstable respectively in the region above or below the transition line appear to agree with theories.

For larger Re accurate numerical results are available. Unfortunately, for larger Reynolds numbers the transition has to be observed so far downstream from the nozzle tip that the small dimensions of the drop rig does not permit us to achieve our goal. More accurate theoretical predictions and experiments over a wider range of flow parameters including small values of (Re, We) near the origin are currently being carried out for a complete delineation of the transition between convective and absolute instabilities.

ROLE OF INTERFACIAL SHEAR

The precise roles of interfacial shear force relative to all other forces in the jet breakup has not

been elucidated (ref. 6). To fill in this information gap, we calculate the power inputs due to all forces which participate in causing the kinetic energy of the disturbance to grow in a volume of the liquid jet. The jet is enclosed by a coaxial circular cylinder. The annular region between the cylinder and the jet is filled with a viscous gas. The relative importance of each force is identified by comparing it with all other forces in the energy budget. The energy budget is obtained by forming the dot product of the linearized Navier-Stokes equations with the velocity perturbation, and then integrating over a given control volume of the liquid jet. The energy budget can be written as

$$KE = PRG + SUT + SHG + SHB + NVG + SHL + NVL + PRL + REY + DIS, \quad (1)$$

Each term in (1) represents the phase averaged time rate of change of physically distinctive factor per unit length of the liquid control volume enclosed by the interface of length λ on the side and by the two circular lids at $z=0$ and $-\lambda$. KE is the time rate of change of the disturbance kinetic energy. The last term DIS is the rate of mechanical energy dissipation through viscosity in the volume, which tends to reduce KE as it is always negative. The energy transfer between the disturbance and the basic flow through the Reynolds stress is represented by REY, the sign of which depends on the flow parameters. The rest of the surface integrals in (1) represent various rates of work done on the control surface. PRG represents the rate of work done by the gas pressure fluctuation on the liquid jet, if it is positive.

If it is negative, the work is done by the liquid jet on the surrounding gas at the expense of the disturbance kinetic energy. The same sign convention is followed by the rest of the work terms. SUT is the rate of work done by the surface tension. SHG is the rate of work done by the shear stress exerted by the fluctuating gas at the interface. SHB is the rate of work done by the shear stress associated with the basic flow distortion caused by the interfacial displacement. NVG represents the rate of work done by the normal viscous stress exerted by the fluctuating gas at the interface. NVL and SHL represent respectively the rates of work done by the normal and tangential components of the viscous stress at the top and bottom ends of the control volume. The rate of the pressure work at the top and bottom ends of the control volume is given by PRL. Each term on the right side of (1) represents a different physical factor which affects the instability of the liquid jet. Therefore the relative magnitude as well as the sign of each term must be evaluated. To achieve this, we must carry out the stability analysis which provides the functions appearing in the integrands of (1). An accurate eigenvector solution is obtained by use of the Chebyshev-collocation method (ref. 15).

Table 1 gives the energy budget of a liquid jet at $Re=1000$, $We=400$, $Q=0.0013$, $N=0.018$, $l=10$, where Q is the gas to liquid density ratio, N is the gas to liquid viscosity ratio, and l is the ratio of the cylinder radius to the jet radius. The wave numbers k_r cover both stable and unstable disturbances. All items are normalized with the energy term of the most amplified disturbance occurring at $k_m = 0.684$. It is seen from this table that the positive rates of change of the disturbance kinetic energy are mainly due to

k_r	KE	REY	SUT	PRL	PRG	NVG	DIS	SHL	NVL	SHG
0.140	0.127	-1.20E-05	0.129	1.59E-05	3.35E-05	9.39E-06	-0.00128	-7.91E-08	2.45E-06	-1.15E-03
0.200	0.248	-2.34E-05	0.254	7.34E-05	-2.06E-04	2.52E-05	-0.00362	-2.25E-07	6.74E-06	-1.78E-03
0.300	0.503	-4.74E-05	0.520	1.81E-04	-3.23E-04	7.95E-05	-0.01130	-6.76E-07	1.97E-05	-2.87E-03
0.400	0.771	-7.21E-05	0.804	4.20E-04	-5.06E-04	1.69E-04	-0.02410	-1.34E-06	3.80E-05	-3.84E-03
0.500	0.980	-9.10E-05	1.030	7.36E-04	-9.49E-04	2.80E-04	-0.04070	-2.10E-06	5.58E-05	-4.52E-03
0.600	1.060	-9.84E-05	1.140	6.50E-04	-1.28E-03	3.89E-04	-0.05920	-2.92E-06	6.54E-05	-4.73E-03
0.684	1.000	-9.31E-05	1.090	1.19E-03	-1.43E-03	4.52E-04	-0.06800	-3.66E-06	6.22E-05	-4.45E-03
0.700	0.973	-9.08E-05	1.060	2.15E-03	-1.45E-03	4.58E-04	-0.07160	-3.80E-06	6.03E-05	-4.34E-03
0.800	0.697	-6.81E-05	0.781	8.82E-04	-1.31E-03	4.33E-04	-0.06810	-4.51E-06	3.98E-05	-3.27E-03
0.900	0.296	-3.47E-05	0.353	4.96E-04	-7.18E-04	2.64E-04	-0.04570	-3.88E-06	1.31E-05	-1.59E-03
1.100	-0.058	3.00E-04	0.067	1.47E-03	-2.71E-03	1.47E-03	-0.12000	-1.09E-05	3.18E-07	-4.76E-03
1.200	-0.160	7.71E-04	0.182	5.79E-03	-6.71E-03	3.36E-03	-0.33400	-3.70E-05	1.05E-06	-1.08E-02

Table 1: Energy budget for Rayleigh mode.
 $Re=1000, Fr^{-1}=0.0, We=400, Q=0.0013, N=0.018, l=10.$

the work done by the surface tension on the control liquid volume. Although the viscous normal stress exerted by gas represented by NVG as well as the normal stress work represented by PRL and NVL at the top and bottom of the cylindrical liquid column also contribute to the growth of the unstable disturbance, they are several orders of magnitude smaller than the surface tension term SUT. The major factor which resists disturbance growth is viscous dissipation. The pressure and the shear stress exerted by the gas at the liquid-gas interface are also significant factors against instability. Although the liquid tangential viscous stress represented by SHL and the bulk Reynolds stress represented by REY also contributed to drain the kinetic energy from the disturbance, they are many order of magnitudes smaller than DIS. However the sum of all negative terms are not sufficiently large in magnitude to counter the destabilizing effect of the surface tension. Thus the mechanism of the instability of a viscous liquid jet in a viscous gas by the Rayleigh mode remains capillary pinching which was demonstrated by Chandrasekhar (ref. 16) who considered an inviscid liquid jet in vacuum. An inviscid Rayleigh jet is neutral with respect to disturbances of wave number larger than the cut off wave number $k_{rc} = 1$. Thanks to viscous dissipation these disturbances are actually damped according to table 1. The stabilizing and destabilizing factors retain their signs in the range of k_r given in table 1, except for the Reynolds stress term. Although some energy is transferred from the mean flow to the disturbances of wavelength shorter than $2\pi R_1$, the growth of these disturbances are nevertheless suppressed by viscous dissipation. Note that the change of SUT with k_r is not monotonic, and its maximum does not occur at k_m . In fact all of the other terms also do not change monotonically, and their maxima do not occur at the same k_r . This indicates the significance of interplay among all items in determining the maximum growth rate.

ACKNOWLEDGMENTS

This work was supported by Grant. No. NAG3-1891 of NASA.

REFERENCES

1. Leib, S.J. and Goldstein, M.E., "The generation of capillary instability on liquid jet," *J. Fluid Mech.* 168, 479-500 (1986).
2. Leib, S.J. and Goldstein, M.E., "Convective and absolute instability of a viscous liquid jet," *Phys. Fluids*, 29, 952-954 (1986).
3. Lin, S.P. and Lian, Z.W., "Absolute instability of a liquid jet in a gas," *Phys. Fluids A*, 1, 490-493 (1989).
4. Lin, S.P. and Lian, Z.W. "Absolute and convective instability of a viscous liquid jet surrounded by a viscous gas in a vertical pipe," *Phys. Fluids. A*, 5, 771-773 (1993).
5. Zhou, Z.W. and Lin, S.P., "Effects of compressibility on the atomization of liquid jets," *J. Propulsion and Power*, 8, 736-740 (1992).
6. Lin, S.P. and Reitz, R.D., "Drop and spray formation from a liquid jet," *Annual Review of Fluid Mechanics* 30, 85-105 (Annual Rev. Inc. Palo Alto, 1998).
7. Chieger, N. and Reitz, R.D., "Regimes of jet breakup and breakup mechanisms (physical aspects)," in *Recent Advances in Spray Combustion: Spray Atomization and Drop Burning Phenomena*, Vol. 1, ed. K.K. Kuo (AIAA Inc. Reston, 1996), pp. 109-135.
8. Lin, S.P., "Regimes of jet breakup and breakup mechanisms (mathematical aspects)," in *Recent Advances in Spray Combustion: Spray Atomization and Drop Burning Phenomena*, Vol. 1, ed. K.K. Kuo (AIAA Inc. Reston, 1996), pp. 137-160.
9. Vihinen, I, Honohan, A.M. and Lin, S.P., "Image of absolute instability in a liquid jet," *Phys. Fluids*. 9, 3117-3119 (1997).
10. Honohan, A.M., "Experimental measurements of the spatial instability of viscous liquid jet at Microgravity," M.S. thesis, Clarkson University, Potsdam, NY 1995.
11. Vihinen, I., "Absolute and convective instability of a liquid jet in microgravity," M.S. thesis, Clarkson University, Potsdam, NY 1996.
12. Lin, S.P. and Creighton, B., "Energy budget in atomization," *J. of Aerosol Sci. And Tech.*, 12, 630-636 (1990).
13. Huerre, P. and Monkewitz, P.A., "Local and global instabilities in spatially developing flows," *Annu. Rev. Fluid Mech.* 22, 473-537 (1990).
14. Monkewitz, P.A., Davis, J., Bojorquez, B. and Yu, M.H., "The breakup of a liquid jet at high Weber number, *Bull. Am. Phys. Soc.* 33, 2273 (1988).
15. Boyd, J.P., Chebyshev and Fourier Spectral Methods, Springer Verlag, New York (1989).
16. Chandreskhar, S., Hydrodynamic and Hydromagnetic Stability, Oxford University Press (1961).